Coupling of ASTEC V2.1 and RASCAL 4.3 codes to evaluate the Source Term and the Radiological Consequences of a Loss-of-Cooling Accident at a Spent Fuel Pool

Antonio Guglielmelli[1]
Italian National Agency for New Technologies, Energy and Sustainable Economic Development (ENEA), Nuclear Safety Division (FSN-SICNUC-SIN)
Via Martiri di Monte Sole 4, 40129 Bologna (BO), Italy
antonio.guglielmelli@enea.it

Stefano Ederli
Italian National Agency for New Technologies, Energy and Sustainable Economic Development (ENEA), Nuclear Safety Division (FSN-SICNUC-SIN)
Via Anguillarese 301, 00123 Roma (RM), Italy
stefano.ederli@enea.it

Fulvio Mascari
Italian National Agency for New Technologies, Energy and Sustainable Economic Development (ENEA), Nuclear Safety Division (FSN-SICNUC-SIN)
Via Martiri di Monte Sole 4, 40129 Bologna (BO), Italy
fulvio.mascari@enea.it

Federico Rocchi
Italian National Agency for New Technologies, Energy and Sustainable Economic Development (ENEA), Nuclear Safety Division (FSN-SICNUC-SIN)
Via Martiri di Monte Sole 4, 40129 Bologna (BO), Italy
federico.rocchi@enea.it

Pietro Maccari
Italian National Agency for New Technologies, Energy and Sustainable Economic Development (ENEA), Experimental Engineering Division (FSN-ING-SIS)
C. R. Brasimone, 40032 Camugnano (BO), Italy
pietro.maccari@enea.it

[1] Corresponding author.

ABSTRACT

This paper deals with a general methodology to evaluate the Source Term (ST) and the Radiological Consequences (RC) of a hypothetical Severe Accident (SA) at a Fukushima-like Spent Fuel Pool (SFP) by coupling ASTEC 2.1 and RASCAL 4.3 SA and consequence projections (CP) codes, respectively. The methodology consists of the following sequential steps: the ST provided by a prior simulation performed by ASTEC V2.1 code was used as input to RASCAL 4.3 code to make a RC analysis. This approach was developed as a preparatory study for the Management and Uncertainties in Severe Accident (MUSA) H2020 European Project, coordinated by CIEMAT, where the ENEA's Nuclear Installations safety laboratory is committed to perform an analysis on a Fukushima-like SFP with the aim to apply innovative management of SFP accidents (WP6) to mitigate the RC of the accident itself. To perform the RC studies that could have an impact on Italy, a Fukushima-like SFP was assumed located in one of the Italian cross-border NPP sites. The weather data adopted are both standard and real hourly meteorological data taken from more than one geographical location. The results of the RC for 96 h of ST release in a range of 160 km from the emission point are reported in terms of Total Effective Dose Equivalent (TEDE), Thyroid dose, and Cs-137 total ground deposition. The mitigating effect on ST and on RC of the cooling spray system (CSS) actuated with several pH values (i.e., 4,7,10) was also investigated.

1 INTRODUCTION

In the last ten years, following the Fukushima Daiichi Nuclear Power Plant (NPP) accident, there was an increase of the research activities devoted to exploring and update the codes capability to calculate the Source Term (ST) [1,2] and the Radiological Consequences (RC) [3,4] of Beyond Design Basis Accidents (BDBA) at Spent Fuel Pool (SFP). The increase attention in assess the code capability to perform a Severe Accident (SA) progression in a NPP and a SFP resulted in the realization of the still in progress Management and Uncertainties of Severe Accidents (MUSA) European H2020 project in

which the authors of this work are involved as official partners. MUSA overall objective is to evaluate the prediction capability of SA codes to modelling reactor and SFP accident scenarios with the quantification of the associated codes uncertainties and the effect of both existing and innovative mitigation strategies on the RC [5]. In this research framework, several studies were also performed for coupling ST and RC codes with the aim to create a comprehensive system capable to make evaluations of all physical quantities involved in the several phases of a SA event: fuel inventory released, time-dependent ST and dose/activity distribution on the surrounding territory. The state of the art of this kind of studies ranges from a simplified approach that involves the use of fast running codes/technics to evaluate the ST and the RC, to an intermediate approach that involves the use of a fast-running code/technique coupled with a dedicate ST or RC code, to a complex approach that includes the use of specifically designed codes both for ST and RC evaluation. In the field of simplified approach, analysis have already been carried out using reactor core inventory as ST and a short-term, short-range, near-surface release gaussian atmospheric dispersion code to evaluate the RC [6]. In the area of intermediate approach, analysis that involves the use of analytic techniques (i.e., technical documents, look up tables, etc.) to evaluate the ST and a more comprehensive Lagrangian atmospheric dispersion code to evaluate the RC were performed [7, 8]. In the field of complex approach, dedicate SA codes to evaluate an accident-related ST and a long range Lagrangian atmospheric dispersion code was used [9]. This study can be considered a contribution in the context of the intermediate approach because involves the use of a specially designed code to model SA phenomena (i.e., ASTEC V2) with a fast-

running code (i.e., RASCAL 4.3) that make the RC consequence by means of a gaussian puff atmospheric dispersion model. This type of coupling has not yet been tested in the scientific research context of coupled ST and RC evaluation systems and it could represent a good compromise between fast and accurate methodologies that could be validate in the next future with benchmarks studies with other types of ST and RC code coupling for furthering check its reliability. Specifically, ASTEC code, has progressively became the European reference code for SA analyses for water cooled reactors [10,11]. ASTEC V2 was developed and extensive validated within the Severe Accident Research NETwork of excellence (SARNET) from 2004 to 2013 within which innovative major improvements such as new core degradation and an in-core 2D magma/debris relocation models were implemented [2]. ASTEC V2.1 also arise from the efforts performed in the Code for European Severe Accident Management (CESAM) European project within which a further improvement of physical modelling (i.e., new core degradation models, Melting Core Concrete Interaction (MCCI) coilability, new reflooding of degrade core model, improving the oxidation of Zircaloy cladding model, new ST evaluation capabilities in both RCS and containment, improving of iodine chemistry modelling) and a validation work was achieved to verify the general capability of ASTEC V2.1 to simulate the state-of-art of the most important SA phenomena particularly relevant in the progression of a SFP and a NPP SA scenario [2]. RASCAL 4 is the official code currently used by United States Nuclear Regulatory Commission (U.S.NRC) emergency operation centre for making dose projections for atmospheric releases during radiological emergencies [12]. RASCAL is included into the Radiation

Protection Computer Code Analysis and Maintenance Program (RAMP) – supported by the U.S.NRC – within the RAMP emergency response category as stand-alone tool for making independent dose and consequences projections during radiological incidents and emergencies [13]. In this work, ldX Eulerian atmospheric dispersion code was also employed to make a preliminary conservative meteo data analysis. ldX is a code specifically developed by the French Institute De Radioprotection et De Sûreté Nucléaire (IRSN) to perform far range radionuclides dispersion analysis into the atmosphere. The model implemented in ldX is like that of Polair3D of the Polyphemus platform and has been validated against the European Tracer Experiment (ETEX), the Algeciras accident, and the Chernobyl accident [14]. The meteo dataset used in this study are all based on the latest fifth major global reanalysis data (ERA5) produced by the European Center for Medium Weather Forecast (ECMWF). The data are stored in ECMWF Meteorological Archival and Retrieval System (MARS) and a pertinent sub-set of the data, interpolated to a regular latitude/longitude grid, are available on the Copernicus Climate Change Service (C3S) [15]. ECMWF operates the C3S on behalf of the European Union (EU) and will bring together expertise from across Europe to deliver the service [16].

The coupling between ASTEC and RASCAL codes was implemented in a serial manner: the ST provided by ASTEC at the end of a simulation was modified in a several parts (i.e., syntax, style, and time step) to be accepted by RASCAL code by means of a python script specifically prepared for this purpose. Subsequently, RASCAL 4.3 was run to perform a RC analysis using as input the ASTEC reworked ST. Therefore, the information between ASTEC and RASCAL was exchanged only at the end of the ASTEC simulation, and no

feedback control was implemented. At the same time, no code coupling was implemented because RASCAL 4.3 can only be used by means of a GUI based interface.

The following section presents the methodology used in this study. In the third section the codes used in this work are discussed with the specific parameters and modules used to perform the analyses. In the fourth section, the results of the application of the ASTEC/RASCAL coupling methodology to a Fukushima-like SFP hypothetically located on one of the Italian cross-border sites are presented. In the last section, some considerations on the results and on the planned future work are reported.

2 METHODOLOGY AND CALCULATION TOOLS

The methodology presented in this study is in principle capable to perform a RC analysis on any nuclear facility; it consists of two steps: ST evaluation with the ASTEC V2.1 code (Study carried out with ASTEC V2, IRSN all rights reserved, [2020]) [17] and RC assessment with the RASCAL 4.3 code [12]. For the present study, ASTEC V2.1 is used to calculate and export a ST resulting from a Loss-of-Cooling SA scenario at a Fukushima-like SFP. Then, the ST file is imported in the RASCAL 4.3 code and the RC consequences are evaluated by means of the Atmospheric Transport module of RASCAL 4.3, according to the user-imposed meteorological conditions. The Fukushima-like SFP model, chosen to perform the ASTEC V2.1 analysis, is an upgraded version of that adopted in the NUGENIA-PLUS AIR-SFP European Project [18] and it will be further developed by ENEA to be used within the MUSA project activities [19]. This activity is developed within the WP6 task of the MUSA project, coordinated by IRSN.

Three meteorological conditions were investigated: RASCAL 4.3 predefined "standard" meteorological data; one point of real 3.456x10+5 s meteorological data located at a specific geographical point where one of the Italian cross-border NPP is located; three additional points of real 3.456x10+5 s meteorological data located far away from the chosen cross-border NPP site. The one point of hourly meteo data located at one of the Italian cross-border NPP was extracted from the history+ Meteoblue online hourly meteo data paid service [20]. The Meteoblue service datasets are based on ERA5 meteorological hourly reanalysis data with a spatial resolution of 3.0x10+4 m and are produced by combining measurement, observation and simulation data and applying data assimilation techniques to achieve the most realistic description of the weather occurrences [21]. The results may be validated and corrected through measurements and observation data, using different post processing techniques like downscaling, statistic, machine learning and nowcasting [22]. The additional three points of hourly meteo data located at about 7.0x10+4 m away from the NPP were extracted from the ERA5 reanalysis database of the Copernicus online service [23]. ERA5 reanalysis method uses the data assimilation principle which combines model data with observations from across the world into a globally complete and consistent dataset using the laws of physics. The ERA5 data used in this study are hourly data on single pressure level with a resolution of 2.5x10+4 m [24]. Figure 1 presents the flow chart of the proposed methodology. All the analyses were performed on a Windows 10 64bit desktop equipped with an Intel Core i7-4710HQ 2.50 GHz and 16 Gb of RAM.

The next two subsections describe the calculation tools (i.e., ASTEC and RASCAL codes) used to evaluate the ST emitted and the RC on the population of the proposed Fukushima-like SFP SA scenario. In detail, the modules and the values of the main parameters assumed in the two codes will be briefly described.

2.1 ASTEC V2.1 code

The Accident Source Term Evaluation Code (study carried out with ASTEC V2, IRSN all rights reserved, [2020]) [2], jointly developed until 2015 by the French "Institut de Radioprotection et de Sûreté Nucléaire" (IRSN) and the German "Gesellschaft für Anlagen und Reaktorsicherheit gGmbH" (GRS), and developed now only by IRSN, aims at simulating an entire SA sequence in nuclear water-cooled reactors from the initiating event through the release of radioactive elements out of the containment. The main uses of ASTEC V2.1 are ST evaluations, accident management studies, and level-2 probabilistic safety assessment (PSA). It features a modular structure where each module is devoted to simulating a specific set of physical phenomena or a specific zone of the NPP. The modelization of the SFP has involved the following modules: CESAR, CPA, ICARE, ISODOP and SOPHAEROS.

CESAR is dedicated to the thermal hydraulic simulation in the primary cooling system (including the vessel) and in the secondary cooling system. It is a system code characterized by a two-phase flow model based on a default five equations approach and, to address the non-equilibrium mechanicals between the liquid and the gas phase, a phase slip model is considered (a six equations model is available in the current version of the code but has not been used in this study). The code adopts a finite

volume discretization approach, which solves the energy and mass conservation equations on the control volume. The time integration is performed using a Newton's method based on a fully implicit scheme [25,26].

ICARE is used to simulate the in-vessel core degradation phenomena. It implements mechanical models, processes several chemical reactions, incorporates FPs release, and describes core thermal behavior, degradation, and relocation in the Lower Plenum (LP), until the rupture of the Lower Head (LH) wall. The code uses basic 2D geometrical objects able to reproduce most of the internals of the core and the related exchange with the coolant fluid, managed by CESAR module. The core radial meshing is based on a multi-channels approach enabling to model, by means of cylindrical concentric fluid channels, the axisymmetric core of a pressurized water reactor (PWR) but also to consider the specific core features of boiling water reactors (BWRs) and pressurized heavy-water reactors (PHWR). The multi-channels approach, allowing the definition of several sub-channels within concentric fluid channels, is also useful to model SFPs [17].

CPA provides a tool based on mechanistic models with the purpose of simulating all the relevant thermal-hydraulic processes and plant states taking place in the containment compartments of a Light Water Reactor (i.e., gas distribution, pressure build up, condensation, hydrogen combustion, etc.). The discretization model adopted is a lumped-parameter one, where the compartments are divided into control volume whose status is defined by the temperature and masses of each component [27].

SOPHAEROS deals with the chemistry and the transport phenomena of the FPs both in the reactor circuits and in the containment. The code divides the main physical and chemical phenomena into two parts: vapor and aerosol phase phenomena. The mass balance equation resulting from the intra-volume phenomena combined with inter-volume transport produce a non-linear system of equations solved by the Newton Raphson method [28].

ISODOP is in charge of calculating FPs decay heat and the isotopes transmutation along the SA sequence [27].

ASTEC V2.1 model of the Spent Fuel Pool

Figure 2 describes the ASTEC V2.1 model of the SFP: it is an extension of the model developed by ENEA in the frame of NUGENIA-PLUS AIR-SFP project [15] which was limited to the simulation of thermal hydraulic and core degradation in a Fukushima-like SFP, accommodating 1525 fuel assemblies (FAs) of different cooling time and burnup. In the developed ASTEC V2.1 model, the 1535 FAs with their racks are divided into 2 groups: the “Hot FAs” which include 548 FAs (21 GWd/MTU) for recently unloaded fuel (i.e., 3.7 months of cooling); and the “Cold FAs” which include 783 FAs (42 GWd/MTU) for the longer stored fuel (i.e., 3.15 years of cooling) plus 204 FAs of fresh fuel (for a total of 987 FAs).

The FAs and racks of the 2 groups are described by ICARE macro-components. The 72 fuel rods of each FA are modelled with a representative cylindrical fuel rod enclosed by the Zr cladding. The Zr water rod, the Zr canister, the steel rack, and the concrete wall of the SFP, are also modelled as ICARE cylindrical structures. Specific

ICARE components are dedicated to the simulation of the steel spacer grids. The floor of the pool was modelled with the ICARE structure dedicated to the LH of the reactor.

The evolution of decay power during the simulated accident transient was computed by ISODOP module and the initial total mass of FPs, assumed in the simulation, is based on the ORIGEN-ARP code [29] calculation of the FPs inventory of recently unloaded and longer stored fuel. The FPs mass was distributed in the “Hot” and “Cold” FAs by means of numerical factors, estimated as a function of decay heat computed by ORIGEN-ARP code, for recently unloaded and longer stored fuel and adjusted to consider the presence of the 204 fresh FAs in the Cold FAs group. In such a way, it has been possible to distinguish the thermal behavior of the two groups of FAs during the simulated accident transient.

The SFP was radially divided into two concentric main fluid channels: “Pool inner channel” and “Pool outer channel” (Fig. 2). The pool inner channel contains 4 additional fluid sub-channels, housing the 2 groups of FAs with their racks. The two concentric sub-channels indicated as “Hot fuel channel” and “Hot bypass channel” (Fig. 2), deal with the Hot FAs. The first one simulates the fluid in the rods bundle and the second the fluid in the gap between the canister and the rack. The same approach is used for the “Cold fuel channel” and “Cold bypass channel” (Fig. 2), dealing with the Cold FAs. The weight of the described channels is based on the number of related assemblies: 548 for the hot channels and 987 for the cold channels.

The 6 SFP fluid channels are connected at the top end with a small CESAR volume, which is used to connect the top part of the pool, with a CPA zone modelling the SFP building.

The SFP building zone is connected to an environment zone, imposing atmospheric temperature and pressure. The CPA SFP building model includes lateral, ceiling, and bottom walls of the containment, to consider a series of physical phenomena such as steam condensation and aerosol deposition.

The Zircaloy oxidation by means of steam and air, the creep and burst of the claddings, the dissolution of UO_2 and ZrO_2 by liquid Zirconium as well as the material melting, and relocation were modelled. The melting temperature of both UO_2 and ZrO_2 were set between 2550 K (solid) and 2600 K (liquid). Oxidation of U-Zr-O in the relocated materials mixture (i.e., MAGMA) is also activated.

The studied accident is a Loss of Cooling without mitigation measures. The simulation starts with a water level which is just at the top of racks, to reduce the computation time.

A Cooling Spray System (CSS) was subsequently added to investigate the mitigation effect of the water on ST emission. The CSS was designed to pump the condensed water located at the bottom of the SFP building in recirculation mode. It was hypothesized that the SFP is connected to a chemical control system thanks to which the pH of the sprayed water can be set by the user. In the calculations the CSS was activated by a water level set point, at about 1.656x10+5 s after the start of the transient and kept working until the end of the calculation.

2.2 RASCAL 4.3 code

The Radiological Assessment System Consequences AnaLysis (RASCAL) [4] code was developed by U.S. Nuclear Regulatory Commission to provide a tool for the rapid

assessment of an incident or accident at any nuclear facility and aid decision making such whether the public should evacuate or shelter in place. RASCAL evaluates time-dependent atmospheric releases (i.e., ST) and dose projection (i.e., RC) from any nuclear facilities that handle nuclear material. The 4.3 version contains new features and revision of several old features (i.e., extension of the domain up to 1.6x10+5 m, increase of the transport time to 3.456x10+5 s, capability to both import and/or merge ST and to evaluate the child thyroid dose) in response to the lessons learned by the U.S. NRC staff after the events at the Fukushima Daiichi NPP. The main new and revised features are consistent with the possibility to evaluate the RC on Italian territory of a hypothetical SA at one of the nearest SFPs. The "Source Term to Dose" (STDose) primary tool was used to evaluate the RC due to a SA scenario by means of some parameter's specifications given as input to a series of sub tools that allow to define the source and location of the radioactive emission, the time-dependent ST, the release conditions, and the meteorological model [12].

The source of the radioactive emission was placed at a SFP according to the case under investigation: a SA event from a Fukushima-like SFP.

In order to locate in space, the user-defined weather data, the position of the SFP was estimated according to a procedure that involves the use of the s.c. surrogate NPP (i.e., plant already available in RASCAL 4.3 database of U.S. plants and which differs from the real plant only in terms of actual power and actual core average burnup) [3,30]. In practice, this means to find among the RASCAL U.S. fleet a BWR-4 Mark-1 plant, which could be used to mock-up the Fukushima-Daiichi NPP unit 4 containing the SFP under SA

conditions. The plant chosen for the analysis is Cooper NPP, a U.S. BWR-4 Mark-1 NPP currently in operation.

The time-dependent ST was imported from ASTEC V2.1 calculation results. The ST time-resolution from ASTEC V2.1 output was set up on a radionuclide emission value every 900 seconds. RASCAL 4.3 allows to use only a subset of the radionuclides evaluated with ASTEC V2.1 code, therefore only the radiological relevant nuclides were imported into RASCAL 4.3 from the ST obtained with ASTEC V2.1.

The dispersion of the radionuclides in the atmosphere during the SA event was evaluated by means of RASCAL 4.3 2-D Gaussian puff model (i.e., TADPUFF) for a distance up to 1.6x10+5 m from the release point for which temporal and spatial variations in meteorological condition are not negligible; the model domain consists of a Cartesian square grid with 41x41 receptor nodes uniformly distributed through the domain itself [31]. The radionuclide atmospheric transport time on the environment was set to 3.456x10+5 s.

RASCAL 4.3 considers the horizontal and vertical radionuclide spread distance dependent from the emission point by means of dispersion parameters (i.e., σ_y, σ_z) which are function of the following variables: friction velocity, mixing layer height, plume height, Monin-Obukhov length and Coriolis factor. These variables exhibit a functional relationship with the dispersion parameters according to the stability class [32,33].

RASCAL includes the two types of radionuclides deposition mechanism. dry deposition (i.e., the uptake at the earth's surface) and wet deposition (i.e., absorption into droplet followed by droplet precipitation or impaction on the earth's surface [34]. Dry deposition is evaluated as the product of a deposition velocity and radionuclide concentration; the deposition velocity is in turn evaluated based on meteo conditions (i.e., stability class), surface roughness (i.e., friction velocity) and wind speed. Typical values of deposition velocity are between 0.0021 and 0.016 m/s for reactive gases, between 0.0031 and 0.0090 m/s for particles and between 0.0014 and 0.0072 m/s for vapor (i.e., I_2) [35].

Wet deposition is assessed using different models for particles and gases. In particular, for particles the wet deposition rate is calculated as the product of a washout coefficient and the overall particles deposition as precipitation falls through the full extent of the plume. The washout coefficient is a function of precipitation type, intensity and, to a limited extent, temperature; typical washout coefficient values are between 0.25 (light rain) and 0.3 (moderate snow). Wet deposition rate for gases is instead evaluated as a product of a solubility coefficient and the rain/snow precipitation rate, assuming that the concentration of gases in the air and in the precipitation are in equilibrium; typical wet deposition velocity is between 2.8x10-5 m/s (light rain) and 4.2x10-4 m/s (moderate snow) [33].

RASCAL 4.3 assumes null dry and wet deposition for nonreactive (CH_3I) and noble gases (Krypton). It also assumes that the atmospheric iodine is made up of 25% particles, 30% vapor (i.e., I_2) and 45% organic form (i.e., CH_3I). This speciation

contributes to the deposition of iodine and to the inhalation doses if ICRP 60/72 dose coefficient are selected, while it does not enter into inhalations doses if ICRP 26/30 dose factors are applied [33].

RASCAL 4.3 model of the meteorological data

In this study, the RC analysis was performed using three different meteorological datasets. The first includes standard time-independent meteorological data as defined within RASCAL 4.3 code. Table 1 reports the first set of RASCAL 4.3 constant "standard" meteorological data.

The second dataset includes one point of actual hourly meteorological data in a time frame of 3.456x10+5 m/s from the start of the ST emission. The starting date of the ST emission was based on a preliminary conservative analysis of the radiological impact on Italian territory of a hypothetical SA at one of the cross-border NPPs using the French Eulerian atmospheric dispersion code ldX, owned by IRSN [14]. The analysis with ldX assumed a "puff" (i.e., 8.64x10+4 s of constant emission) release of I-131 (i.e., 1.0x10+17 Bq) for a transport time of 3.456x10+5 s using an operational meteorological dataset provided by Météo France and available in a range of ten years (i.e., 2002-11) on the so-called ARPEGE domain (resolution 5.0x10+4 m). The most conservative start date obtained for one of the neighboring sites is: 2002-12-25 at 09:00 p.m. This dataset was located on the NPP site, and it was extracted from the on-line history+ Meteoblue

paid service [20]. Table 2 reports some date-related values of the dataset of hourly meteo data.

The stability class was evaluated using wind speed, solar radiation and cloud cover hourly data according to Pasquill-Gifford classification [32]. The wind speed for each hourly meteo data was set by means of two values: average wind for the first 2.7x10+3 seconds and gust wind for the second 9.0x10+2 seconds. Figures 3-4 report the wind rose and the wind velocity distribution within 3.456x10+5 s from the emission date (i.e., 25-12-2002) using the second meteo dataset.

According to the Meteoblue service definition for which the wind rose displays the direction in which the wind blows, the prevailing winds directions come from N, NNE, NE and account for up to 70% of the total wind directions; the highest wind speed values come from NNE, NE and WSW with an average value of 4.0 m/s. The difference between gust and average wind in the overall time frame is between a factor 1 and 10 (Fig. 4).

The second, third and fourth datasets used in this study also include actual hourly meteorological data in a time frame of 5.76x10+3 s from the start of the hypothetical ST emission from NPP site. The three datasets are all located at about 7.0x10+3 m away from the NPP, but the second and the third ones – here referred as north and south dataset – are shifted of ±20° with respect to the geographical location of the fourth one, here referred as central dataset. This choice has allowed to define hourly meteo information in areas of the geographical domain that are at 2.5 computational cells from the location of the central dataset, being the RASCAL computational cells dimension

equal to 8.0x10+3 m. The meteo dataset were extracted from ERA5 hourly data available for free within the Copernicus European service [23]. ERA5 is the fifth generation of European Centre Medium Weather Forecast (ECMWF) meteo data reanalysis of the global climate and weather [24]. The meteo data were downloaded in a Network Common Data Form (i.e., *.nc file format) and the single hourly weather variables (i.e., wind velocity, wind speed, temperature, solar radiation, precipitation) were extracted for each of the three datasets (i.e., central, north, and south) by means of a python script specifically implemented for this work. The stability class was once again evaluated using wind speed, solar radiation and cloud cover hourly data according to Pasquil-Gifford classification [32]. The cloud cover hourly data was taken from a free online service [36]. Tables 3-5 reports some date-related hourly parameters of the three datasets.

In order to evaluate if the three geographical points on which the meteo data were extracted are located quite far from each other to produce detectable differences on the meteo data field, the time dependent trend of the wind speed and wind direction of the central, north and south datasets were compared (Figs. 5-6). The convention adopted for the wind direction is equal to that used by RASCAL 4.3: clockwise with the zero set in the compass southern direction that is the direction on which the wind - that comes from north - arrives.

The intercomparison of the three datasets of wind speed and direction showed in some time range not negligible relative difference, also more than ±10%, with respect to the central dataset. In detail, the relative differences of north wind direction data are

more than ±10% for the following time frames: six h starting from 15:00 on 26/12/02, eleven h starting from 00:00 on 28/12/02, 2.16x10+4 s starting from 16:00 on 28/12/02, 2.88x10+4 s starting from 06:00 on 29/12/02. The relative differences of south wind direction are also more than ±10% for the following time frame: 4.34x10+4 s from 03:00 on 29/12/02. Moreover, the relative difference of north and south hourly wind direction data that overruns a relative difference of ±10% are 38.1% and 39.2% respectively. The evaluation of the wind roses of the three locations where the hourly meteo data were located, also provided a qualitative estimation of the difference between each of the three meteo dataset (Figs. 7-9).

3 RESULTS AND DISCUSSIONS

The first set of results is the ST generated by ASTEC code. Figure 10 shows the time-dependent ST produced from a series of radionuclides (RNs) released from the SFP since the start of release in atmosphere (i.e., 4.32x10+5 s) for 3.456x10+5 s of emission time. The RNs list (i.e., Cs-134, Cs-136, Cs-137, I-131, Kr-85, Pu-238, Ru-106, Sr-90, Y-90) is the list of radionuclides with the greatest radiological impact potentially emitted from a SFP as assessed by IRSN and ENEA within the MUSA Project activities [5]. Figure 7 reports the contribution to the ST of all radionuclides included in the RNs list with the exclusion of Pu-238 for which ASTEC provides the first release in atmosphere only after 10 days from the start of the SA event at the SFP, time for which it is reasonable to assume that all the necessary emergency response countermeasures have already been implemented.

Figure 10 also shows that the most important radionuclides release occurs between 2.628x10+5 and 2.988x10+5 safter the start of atmospheric emission and that all the radiologically important RNs reach a saturation value ten h before the end of the RASCAL 4.3 calculation. However, Y-90 presents a residual activity of 4.4x10+16 Bq until the end of the imposed ASTEC simulation; this activity could be potentially released before the adoption of emergency countermeasures. Nevertheless, ENEA contribution on the RNs list assessment found that Y-90 is a contributor for groundshine exposition mode only with, in addition, a negligible weight (<1%) compared to the other radiological relevant radionuclides. Therefore, neglecting the residual 4.4x10+16 Bq activity not considered in the RASCAL calculation does not introduce an appreciable error in the RC assessment.

The second set of results is the evaluation of the mitigation effect of the CSS actuated with several pH values on the ST generated by each of radionuclides belonging to the RNs list. Figures 11 reports the reduction effect due to the activation of the CSS for several pH values on I-131, being in the ASTEC modelling the other radionuclides included in RN list are not affected by the pH of the water. Figure 11 also accounts for a decrease of the I-131 released activity as water pH increases; this phenomenon essentially depends on the pH-related behavior of two chemical reactions involved in the water phase chemistry: the increase of I_2 hydrolysis and of the HOI disproportionation as the pH value increase [37, 38].

The third set of results is the RC due to the atmospheric transport of the evaluated ST with real, site-related hourly meteorological dataset located in one and four points of

the geographical domain, respectively. The adoption of one-point hourly meteo data has allowed to evaluate the effect of time-dependent weather conditions on the final RC results (Figs. 14,17,20); the adoption of four-point hourly meteo dataset has allowed to assess the effect of time-dependent and space-dependent weather conditions on the RC results (Figs. 15,18,21) and to compare the four-point meteo data with the one-point meteo data RC results.

The intercomparison between one point and four-point meteo data fields (Figs. 12-13) on a fixed date emphasizes that the adoption of a more refined meteo field (Fig. 13) allows to perform RC analysis with RASCAL 4.3 in a more realistic situation with a non-uniform wind field and meteo parameters (i.e., stability, precipitation, mixing heights) on the 2D domain. The topography adopted in the simulation is related to the surrogate Cooper NPP plant.

Figures 14-16 report both TEDE, thyroid dose and Cs-137 total ground deposition distribution maps for the most conservative SA scenario (i.e., Sprays not activated). The inhalation dose factor used on the calculation are based on the recommendation of the International Commission on Radiological Protection (i.e., ICRP 60/72) [39]. An intercomparison with the distribution maps achieved with the RASCAL 4.3 standard Meteorology data is also reported. The maps reveal that the SE-SSE is the direction of the most impacted zone according to the direction from which the wind blow (i.e., 300-350 rad) in the timeframe (i.e., 2.628x10+5 – 3.132x10+5 s) of the maximum radiological emission (Fig. 3). In general, a significant impact of different meteorological conditions and ST emission time on both the distribution of the dose and the total ground

deposition was noticed. For the Total Effective Dose Equivalent (TEDE) scenario and with respect to the application of the standard meteo dataset, the one point of actual meteo data reduce the radionuclides spread into the atmosphere from more than 1.6x10+5 m to about 1.0x10+5 m (Fig. 14), the adoption of four-point actual meteo data further reduce the radionuclides spread at about 8.0x10+4 m (Fig. 15). Figures 14-19 report a legend with a dose range split according to early phase criteria of the Protection Action Guide (PAG) implemented by U.S. Emergency Protection Agency (EPA) [40]. For the specific SA scenario and meteo data implemented in this study, RASCAL 4.3 foresees the adoption of some early phase protective actions (i.e., sheltering-in-place or evacuation of the public) in the SE-SSE directions up to 1.1x10+5 m from the emission with a one-point hourly meteorology data (Fig. 14). The insertion of other three point of 3.456x10+5 s of actual meteo data produced a reduction of the distance to which early protective action should be adopted up to 6.0x10+5 m (Fig. 15).

The second set of evaluated results are the thyroid dose distribution for adult population, being this radiological parameter one of the main indicators consider by stakeholders to evaluate the adoption of possible emergency countermeasure in an early phase of a SA scenario (Figs. 17-19).

The evaluation of Cs-137 total ground deposition was also performed with the aim to have an assessment of the late consequences of the Fukushima-like SFP severe accident scenario (Figs. 20-22). Figures 20-22 highlight that — regardless of the meteo data scenario (i.e., standard, one point, four points meteo data) considered in this study — the Cs-137 total ground deposition alone involves the adoption of late countermeasures

up to a distance greater than 1.6x10+5 m; in fact, the total ground deposition exceeds in all the involved cells the maximum level allowed by the European Union for leaf vegetables (i.e., 2500 Bq/m^2) [41].

The computational time required to perform a RC analysis with increasingly detailed meteo data was also compared (Tab. 6). The results showed that also the time required to perform an RC analysis with the more complex meteo dataset (i.e., four actuals 3.456x10+4 s meteo data points) is consistent with emergency preparedness activities for which it is crucial to realize a RC analyses in a fast-running mode. Table 7 summarizes the several ST and RC cases analyzed in this study with the associated main parameters options.

4 CONCLUSIONS

In this paper, a general methodology to evaluate the RC due to a hypothetical SA scenario at a Fukushima-like SFP was proposed. This methodology can be considered an additional contribute to the intermediate approach research field of the ST and RC codes coupling and it will allow future benchmark studies with the other types of ST and RC codes coupling system. It also lets to make a more precise evaluation of the RC with respect to the use of a stand-alone radiological impact assessment code because it combines a code specifically designed to estimate the ST during a SA (i.e., ASTEC v2.1) with a validated and widely used fast-running code for RC analysis (i.e., RASCAL 4.3). The preliminary application of this methodology on an Italian cross-border site, where it is

hypothesized that a Fukushima-like SFP is positioned, has highlighted the relevant impact of ST temporal dynamic on the final spatial dose distribution. The adoption of increasingly refined meteo datasets (i.e., from standard to four points of hourly meteo data) caused a reduction of the distance from the emission point at which non negligible radiological effects could occur. If countermeasures are activated and/or effective to stop the SFP release three days before the emission start, the adoption of a classical mitigation strategy (i.e., spray system) has revealed that a chemically basic environment seems capable of reducing the RC resulting from the major contributors to the dose (i.e., I-131), being I-131 the only radionuclide, among them, to be affected by water pH value in the ASTEC modelization. In the future this methodology will be applied to a real European SFP placed in one of the Italian cross-border NPP sites, together with actual terrain roughness and morphology data of the site itself, and with time-dependent weather data on more than four points of the geographical domain.

ACKNOWLEDGMENTS

The authors would like to thank Dr. Antonio Cervone ENEA researcher of the FSN-SICNUC-SIN laboratory for the support given in obtaining the ERA5 meteo data from the Copernicus online database service.

FUNDING

This project has received funding from the Euratom research and training programme 2014-2018 under grant agreement No. 847441.

REFERENCES

[1] Nuclear Energy Agency, Committee on the Safety of Nuclear Installation. Status Report on SFPs under Loss-of-Cooling and Loss-of-Coolant Accident conditions, Technical report NEA/CSNI/R(2015)2, May 2015, 203 pages. Free download from:

https://www.oecd-nea.org/jcms/pl_19596/status-report-on-spent-fuel-pools-under-loss-of-coolant-accident-conditions-final-report?details=true

[2] Nowack H., Chatelard P., Chailan L., Hermsmeyer St., Sanchez V., Herranz L., 2018. CESAM - Code for European Severe Accident management, EURATOM project on ASTEC improvement, Annals of Nuclear Engineering, Vol. 116, pp. 128-136.

[3] Guglielmelli G., Rocchi F., 2014. FAST-1: Evaluation of the Fukushima Accident Source Term through the fast-running code RASCAL 4.2: Methods & Results, ENEA technical report, UTFISSM-P000-017, 24 pages. Free download from:

https://iris.enea.it/retrieve/handle/20.500.12079/7612/1275/UTFISSM-P000-017_rev.1.pdf

[4] Ramsdell J. V., Athey G. F., McGuide S. A., Brandon L. K., 2012. RASCAL 4: Description of Models and Methods, U.S. Nuclear Regulatory Commission, Office of Nuclear Security and Incident Response, NUREG-1940, 225 pages. Free download of content:

https://www.nrc.gov/docs/ML1303/ML13031A448.pdf

[5] https://musa-h2020.eu/objectives/; Accessed April 6, 2022.

[6] Obeng H. K., Birikorang S. A., Gyamfi K., Adu S., Nyamful A., 2021. Assessment of radiological consequence of a hypothetical accident at the Ghana Research Reactor-I facility based on terrorist attack, Science Progress, Vol. 104(4), pp. 1-24. Free download from:

https://journals.sagepub.com/doi/pdf/10.1177/00368504211054986

[7] Pappas C., Ikonomopoulos A., Sfetsos A., Andronopoulos S., Varvayanni M., Catsaros N., 2014. Derivation of the source term, dose results and associated radiological consequences for the Greek Research Reactor - 1, Nuclear Engineering and Design, Vol. 274, pp. 100-117.

[8] Raja Shekhar S.S., Venkata Srinivas C., Rakesh P.T., R. Venkatesan, Venkatraman B., 2020. Radiological consequence assessments using time-varying source terms in ONERS- decision support system for nuclear emergency response, Progress in Nuclear Energy, Vol. 127, 103436.

[9] Kim S., Lee K., Park S., Han S., Ahn K., Hwang S., 2022. Interfacing between MAAP and MACCS to perform radiological consequences analysis, Nuclear Engineering and Technology, Vol. 54, No. 4, pp. 1516-1525.

[10] Van Dorsselaere J. P., Auviens A., Beraha D., Chatelard P., Herranz L. E., Journeau C., Klein-Hessling W., Kljenak I., Miassoedov A., Paci S., Zeyen R., 2015. Recent severe accident research synthesis of the major outcomes from the SARNET network, Nuclear Engineering and Design, Vol. 291, pp. 19-34.

[11] Mascari F., De La Rosa Blul J. C., Sangiorgi M., 2019. Analyses of an Unmitigated Station Blackout Transient in a Generic PWR-900 with ASTEC, MAAP and MELCOR Codes", NUREG/IA-0515.

[12] Ramsell J. V., Jr., Athey G. F., Rishel J. P., 2015. RASCAL 4.3: Descriptions of Models and Methods, NUREG-1940, Supplement 1. Free download from:

https://www.nrc.gov/docs/ML1303/ML13031A448.pdf

[13] https://ramp.nrc-gateway.gov/topic/emergency-response-codes; Accessed April 6, 2022

[14] Tombette M., Quentric E., Quelo D., Benoit J.P., Mathieu A., Korsakissok I., Didier D., 2014. C3X: a software platform for assessing the consequences of an accidental release of radioactivity into the atmosphere, Poster presented at Fourth European IRPA Congress, 23-27 June 2014, Geneva.

[15] https://confluence.ecmwf.int/display/CKB/ERA5%3A+data+documentation; Accessed April 6, 2022.

[16] https://cds.climate.copernicus.eu/about-c3s; Accessed 6, 2022.

[17] Chatelard P., Belon S., Bosland L., Carénini L., Coindreau O., Cousin F., Marchetto C., Nowack H., Piar L., Chailan L., 2016. Main modelling features of the ASTEC V2.1 major version, Annals of Nuclear Energy, Vol. 93, pp. 83-93.

[18] Coindreau O., Jackel B., Rocchi F., Alcaro F., Angeloza D., Bandini G., Barnak M., Behler M., Da Cruz D. F., Dagan R., Drai P., Ederli S., Herranz L. E., Hollands T., Horvath G., Kaliatka A., Kljenak I., Kotsuba O., Lind T., Lopez C., Mancheva K., Matejovic P., Matkovic M., Steinbruck M., Stempniewicz M., Thomas R., Vileiniskis V., Visser D. C., Vokàc P., Vorobyov Y., Zhain O., 2018. Severe accident code-to-code comparison for two accident scenarios in an SFP, Annals of Nuclear Energy, Vol. 120, pp. 880-887.

[19] Herranz L. H., Beck S., Sànchez-Espinoza V. H., Mascari F., Brumm S., Coindreau O., Paci S., 2021. The EC MUSA Project on Management and Uncertainty of Severe Accidents: Main Pillars and Status, *Energies*, Vol. *14*, 4473. Free download from:

https://www.mdpi.com/1996-1073/14/15/4473.

[20] https://www.meteoblue.com/it/historyplus; Accessed April 6, 2022.

[21] https://content.meteoblue.com/en/specifications/data-sources/weather-simulation-data/reanalysis-datasets; Accessed April 6, 2022.

[22] https://content.meteoblue.com/en/specifications/data-sources; Accessed April 6, 2002

[23] https://cds.climate.copernicus.eu/#!/search?text=ERA5&type=dataset; Accessed April 6, 2022.

[24] https://cds.climate.copernicus.eu/cdsapp#!/dataset/reanalysis-era5-single-levels?tab=overview; Accessed April 6, 2022.

[25] Gómez-García-Toraño I., Laborde L., 2018. Validation of the CESAR friction models of the ASTECV2.1 code based on Moby Dick experiments, Journal of Nuclear Engineering and Radiation Science, Vol 5, No. 2, pp. 1–9.

[26] Gómez-García-Toraño I., Laborde L., Zambaux J., 2018. Overview of the CESAR thermohydraulic module of ASTEC V2.1 and selected validation studies, Proceedings of the 18th International Youth Nuclear Congress (IYNC2018), Bariloche, Argentina, pp. 11–17.

[27] Cantrel L., Cousin F., Bosland L., Chevalier-Jabet K., Marchetto C., 2014. ASTEC V2 severe accident integral code: Fission product modelling and validation, Nuclear Engineering and Design, Vol. 272, pp. 195-206.

[28] Cousin F., Dieschbourg K., Jacq F., 2008. New capabilities of simulating fission product transport in circuits with ASTEC/SOPHAEROS v.1.3, Nuclear Engineering and Design, Vol. 238, No. 9, pp. 2430-2438.

[29] Rearden B. T., Jessee M. A., 2018. SCALE Code System, ORNL/TM-2005/39, Version 6.2.3, 2764 pages. Free download of content:

https://www.ornl.gov/sites/default/files/SCALE_6.2.3.pdf

[30] Guglielmelli A., Rocchi F., 2017. Evaluation of the radiological impact on the Italian territory of a SA at Krško NPP by means of a statistical methodology, Proceedings of the 26th International Conference Nuclear Energy for New Europe (NENE2017), Bled, Slovenia, September 11 14, 2017, Paper 806, 9 pages. Free download from: https://arhiv.djs.si/proc/nene2017/html/pdf/NENE2017_806.pdf

[31] Athey G. F., Brandson L. K., Ramsdell J. V., Jr., 2013. RASCAL 4.3 Workbook, U. S. Nuclear Regulatory Commission, Office of Nuclear Regulatory Research, 247 pages. Free download of content: https://www.nrc.gov/docs/ML1328/ML13281A475.pdf

[32] Edokpa D. O., Nwagbara M. O., 2017. Atmospheric Stability Pattern over Port Harcourt, Nigeria, Journal of Atmospheric Pollution, Vol. 5, No. 1, pp. 9-17. Free download from:

http://www.sciepub.com/abstract/abstract.aspx?id=jap&num=7265

[33] Ramsdell J.V., Jr., 2014. RASCAL 4.3 Dispersion and Deposition Models, 18th Annual George Mason University Conference on Atmospheric Transport and Dispersion Modeling, Fairfax, Virginia, U.S.A. Free download from:

https://www.icams-portal.gov/meetings/atd/gmu2014/pdf/04-GMU_Ramsdell_RASCAL-4-3_Dispersion-and-Iodine-Models.pdf

[34] Zanetti P., 2013. Air Pollution Modeling: Theories, Computational Methods and Available Software, Springer, pp. 249-262.

[35] Rossi F., Guglielmelli A., Rocchi F., 2015. Impact of a security event at a TRIGA reactor, Annals of Nuclear Energy, Vol. 76, pp. 125-136.

[36] https://www.wunderground.com; Accessed April 6, 2022

[37] Ashmore C.B., Gwyther J.R., Sims H. E., 1996. Some effects of pH on inorganic iodine volatility in containment, Nuclear Engineering and Design, Vol. 166, No. 3, pp. 347-355.

[38] Bosland L., Cantrel L., Girault N., Clement B., 2010. Modeling of iodine radiochemistry in the ASTEC code: description and application to FPT-2 Phebus test, Nuclear Technology, Vol. 171, No. 1, pp. 88-107.

[39] Beninson D., Jammet H., Smith H., 1991. 1990 Recommendation of the International Commission on Radiological Protection, ICRP Publication 60, Pergamon Press, 211 pages. Free download of content:

https://journals.sagepub.com/doi/pdf/10.1177/ANIB_21_1-3

[40] Domenech H., 2020. Radiation Safety, Management and Programs, Springer (USA), Chapter 16.

[41] Presidenza del Consiglio dei Ministri, Dipartimento della Protezione Civile, CEVaD, 2010. Manuale per le Valutazioni Dosimetriche e le Emergenze Ambientali, 122 pages. Free download of content:

https://www.isprambiente.gov.it/files/pubblicazioni/manuali-lineeguida/3447_MLG_57_2010.pdf

NOMENCLATURE

ARPEGE	Action de Recherche Petite Echelle Grande Echelle
ASTEC	Accident Source Term Evaluation Code
BDBA	Beyond Design Basis Accidents
BWR	Boiling Water Reactor
CESAR	Primary and secondary cooling system thermoydraulic module of ASTEC code
CP	Consequence Projections

CPA	Containment thermoydraulic module of ASTEC code
CSS	Cooling Spray System
C3S	Climate Change Service
ECMWF	European Center for Medium Weather Forecast
ENEA	Italian National Agency for New Technologies, Energy and Sustainable Economic Development
ERA5	Fifth major global reanalysis data produced by ECMWF
ETEX	European Tracer Experiment
EU	European Union
EPA	Emergency Protection Agency
FA	Fuel Assembly
FSN-SICNUC-SIN	Laboratory for the Safety of Nuclear Installations of ENEA Fusion and Nuclear Security department
GRS	German Gesellschaft für Anlagen und ReaktorSicherheit
ICARE	In-vessel core degradation module of ASTEC code
ICRP	International Commission on Radiological Protection
IRSN	Institute De Radioprotection et De Sûreté Nucléaire
ISODOP	Isotopes time-dependent activities and decay heat module of ASTEC code
ldX	Long distance eulerian atmospheric dispersion code
LH	Lower Head
LP	Lower Plenum
MARS	Meteorological Archival and Retrieval System

MCCI	Melting Core Concrete Interaction
MUSA	Management and uncertainties in Severe Accident
NPP	Nuclear Power Plant
NUGENIA-PLUS AIR-SFP	Nuclear GENeration II & III Association: AIR-SFP project
ORIGEN-ARP	Isotopic depletion and decay analysis code using problem-dependent cross sections generated by Automatic Rapid Processing module
PAG	Protection Action Guide
PSA	Probabilistic Safety Assessment
PHWR	Pressurized Heavy Water Reactor
PWR	Pressurized Water Reactor
RAMP	Radiation protection computer code Analysis and Maintenance Program
RASCAL	Radiological Assessment System Consequences Analysis
RC	Radiological Consequences
RN	Radionuclide
SA	Severe Accident
SARNET	Severe Accident Research NETwork of excellence
SFP	Spent Fuel Pool
SOPHAEROS	Fission product transport module of ASTEC code
ST	Source Term
TEDE	Total Effective Dose Equivalent
U.S.NRC	United States Nuclear Regulatory Commission

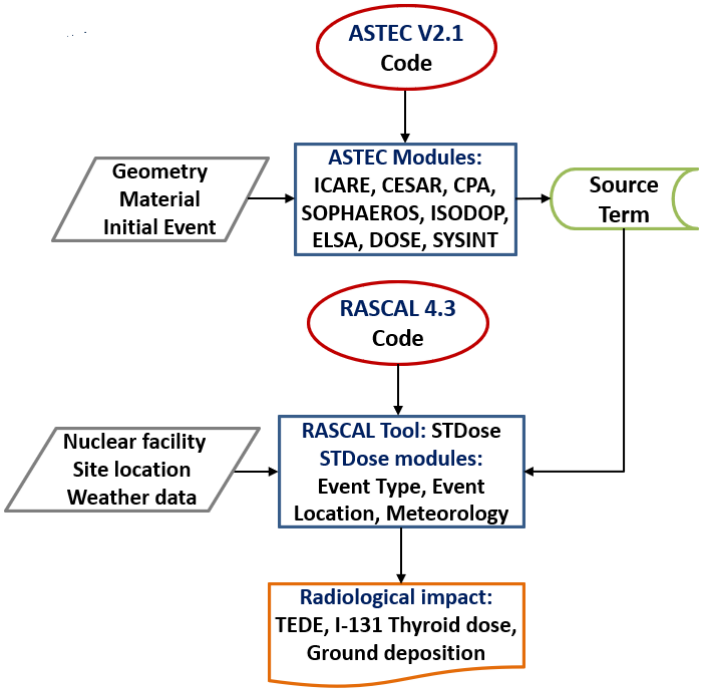

Figure 1: Flow chart of the methodology to evaluate the RC from ASTEC-RASCAL coupling

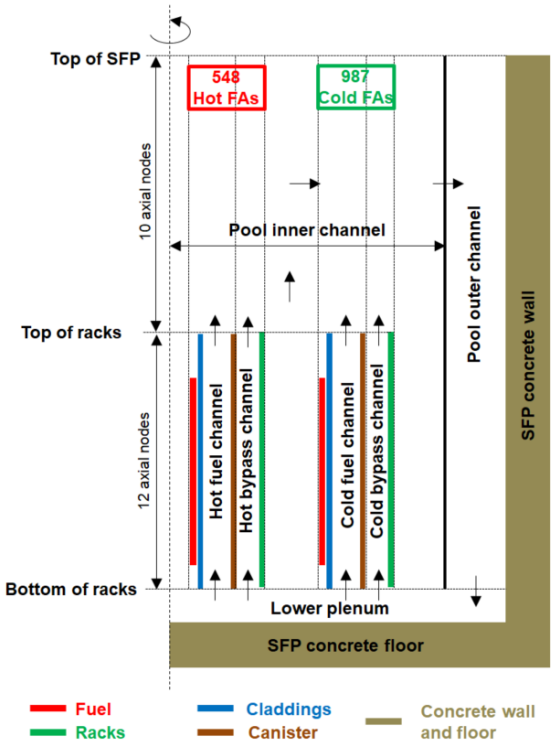

Figure 2: Axial view of the Fukushima-like SFP model – ASTEC code

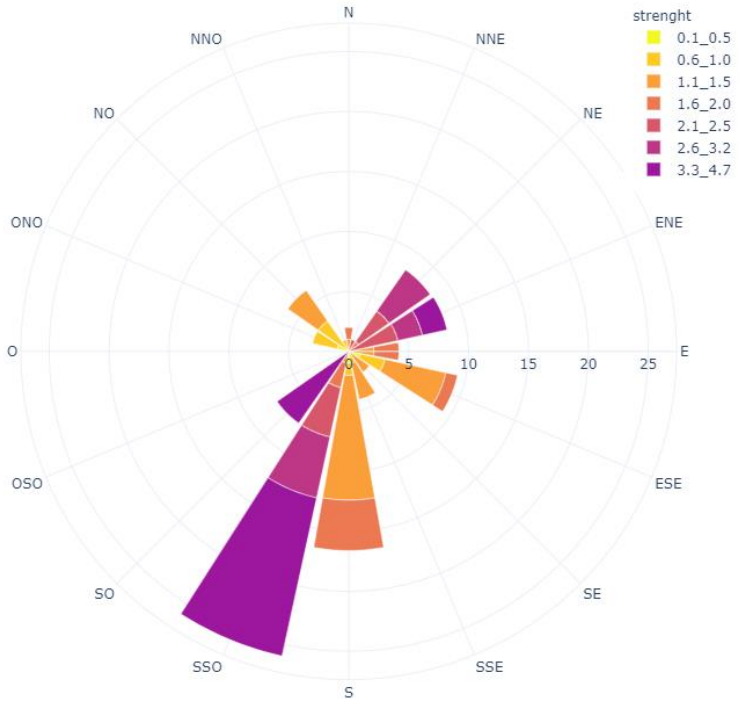

Figure 3: Wind rose on the SFP - Meteoblue data

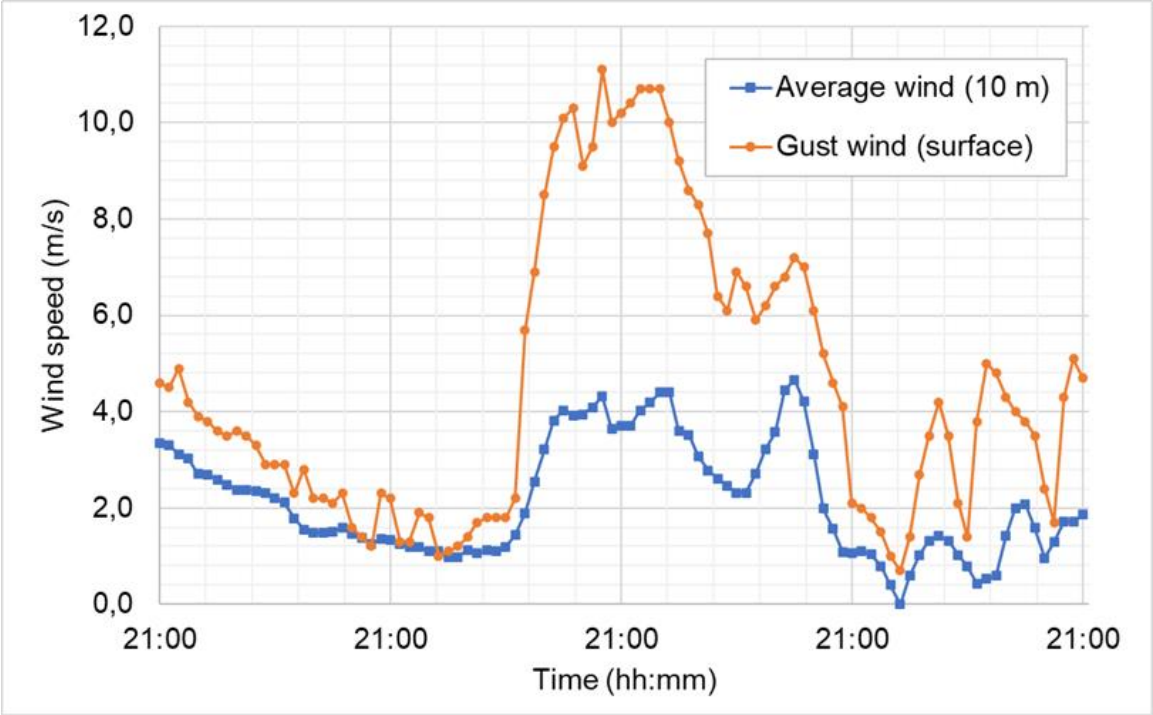

Figure 4: Average and gust wind – Meteoblue data

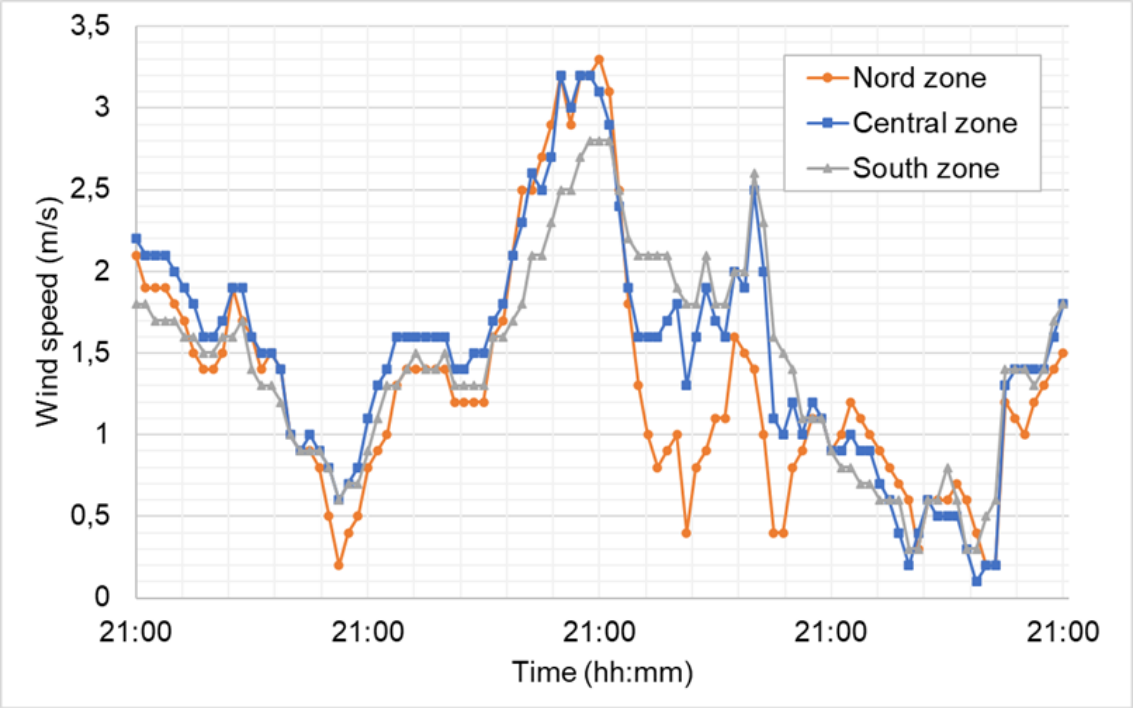

Figure 5: Comparison of the wind speed vs time of the three meteo dataset – ERA5 data

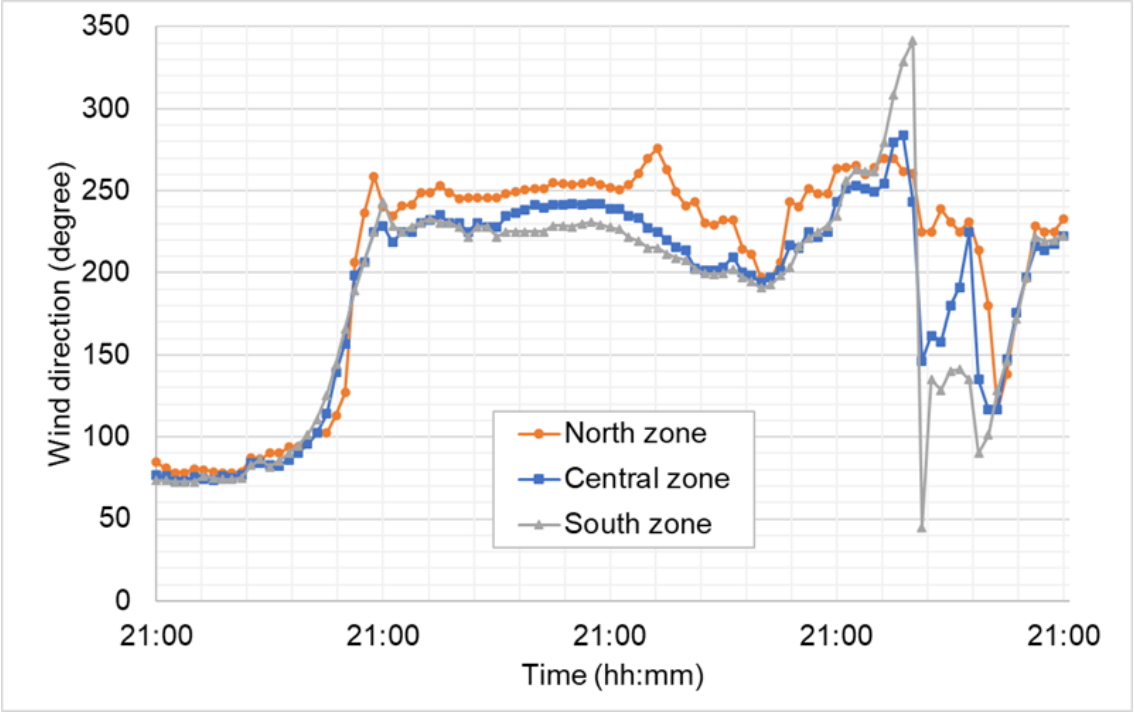

Figure 6: Comparison of the wind direction vs time of the three meteo dataset – ERA5 data

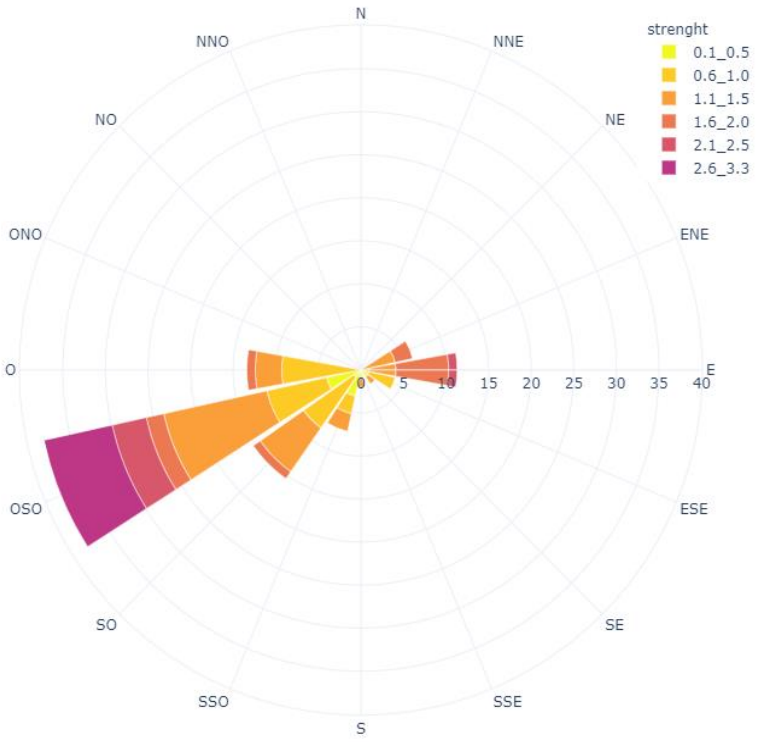

Figure 7: Wind Rose of the North Point – ERA5 meteo data

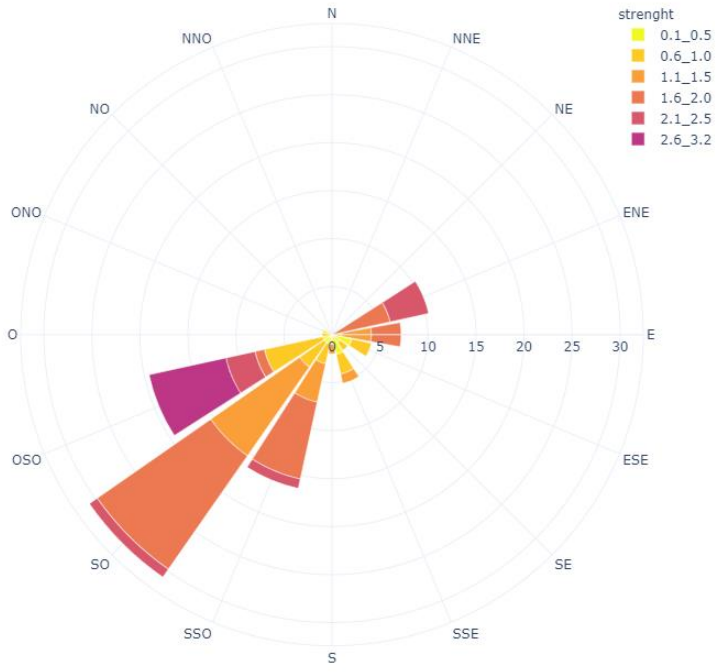

Figure 8: Wind Rose of the Central Point – ERA5 meteo data

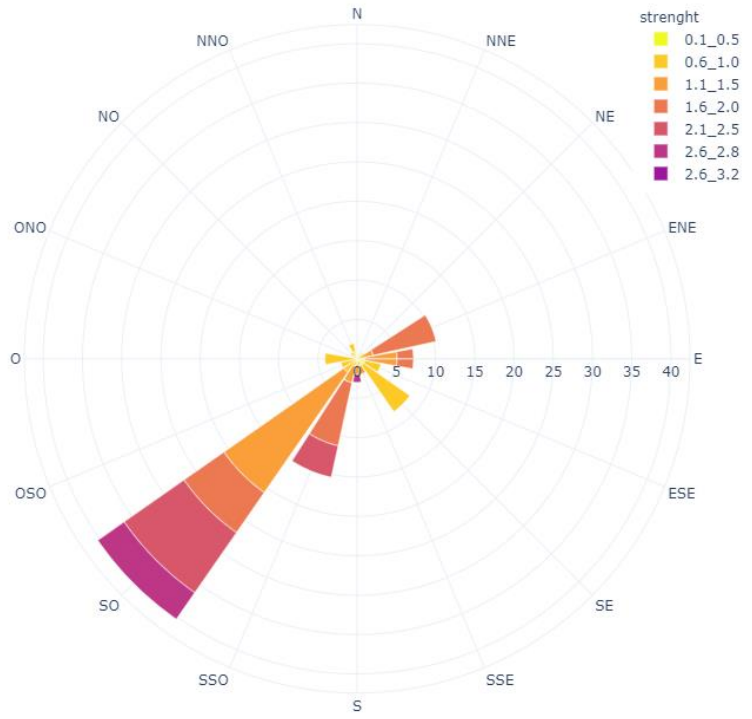

Figure 9: Wind Rose of the South Point – ERA5 meteo data

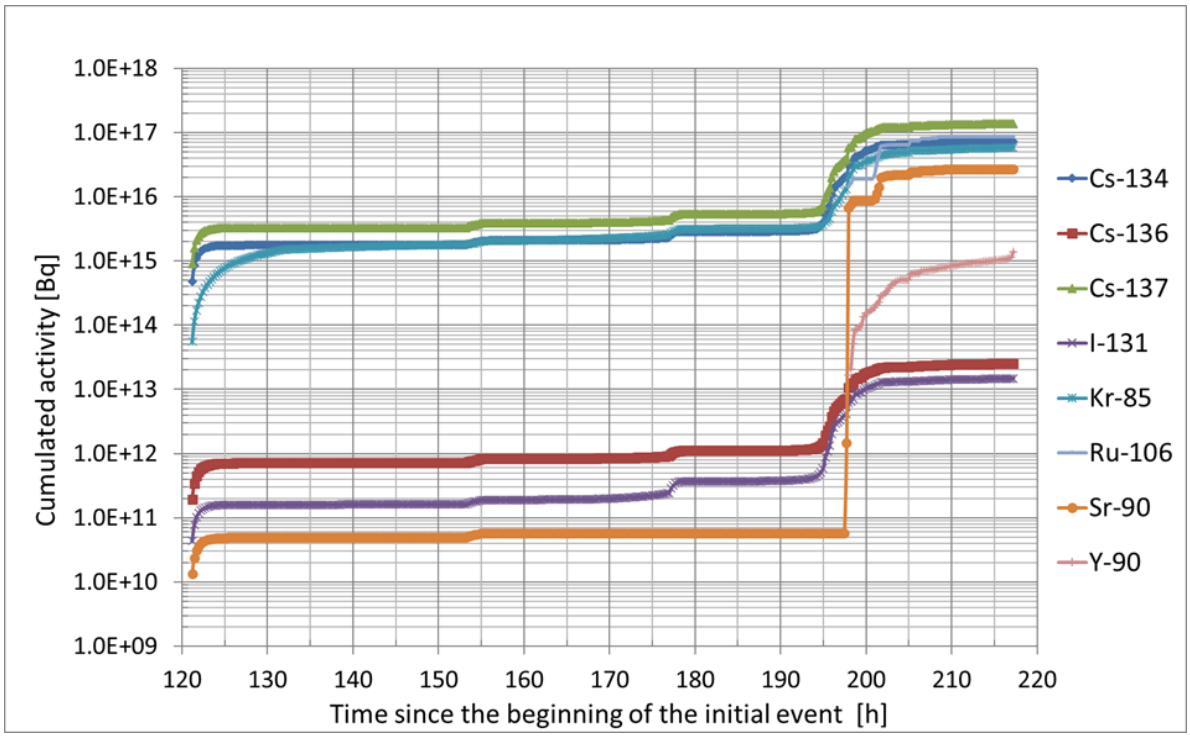

Figure 10: ST emitted from SFP during a Loss-of-Coolant accident scenario – ASTEC code

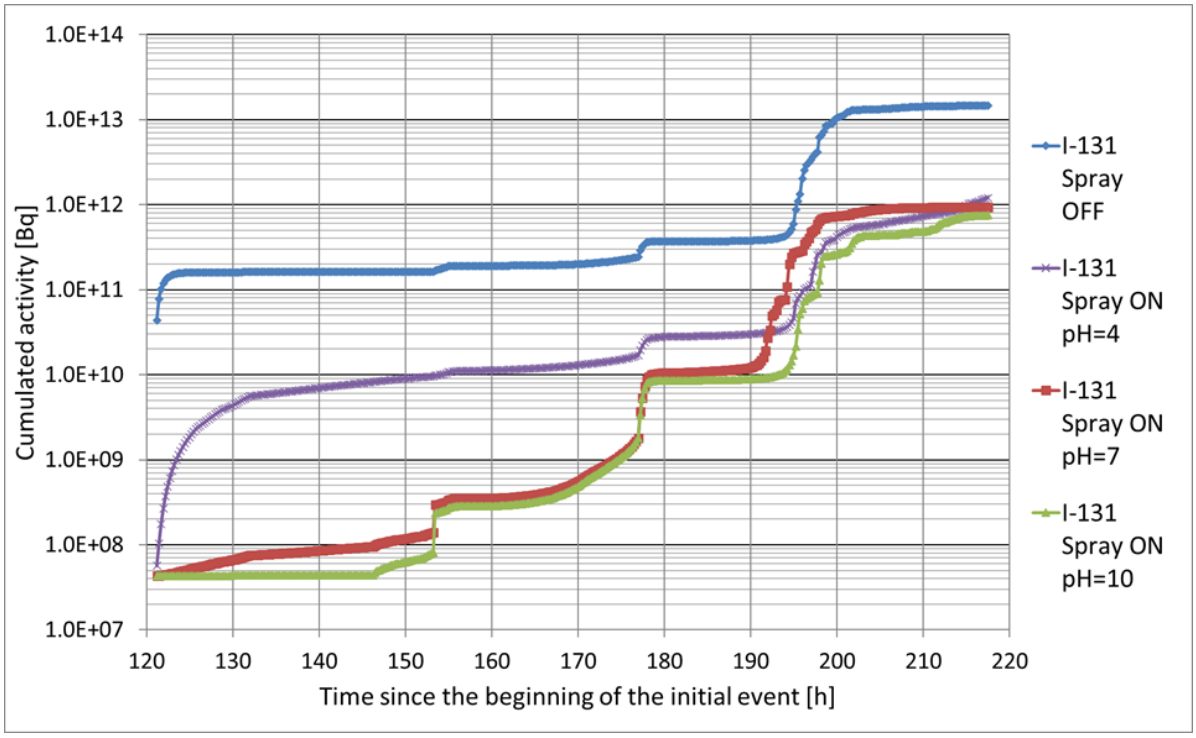

Figure 11: I-131 ST for several mitigation conditions (Spray: OFF/ON, pH: 4,7,10)

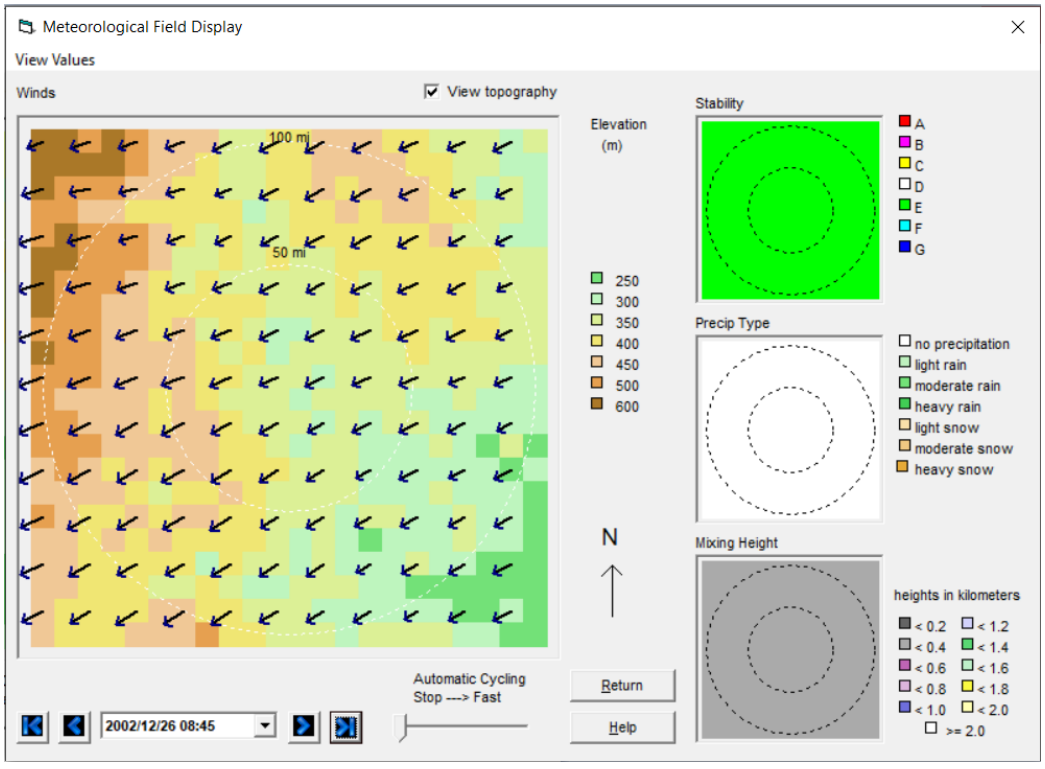

Figure 12: Meteorological data with one-point meteo data, 2002/12/26 08:45 – RASCAL 4.3

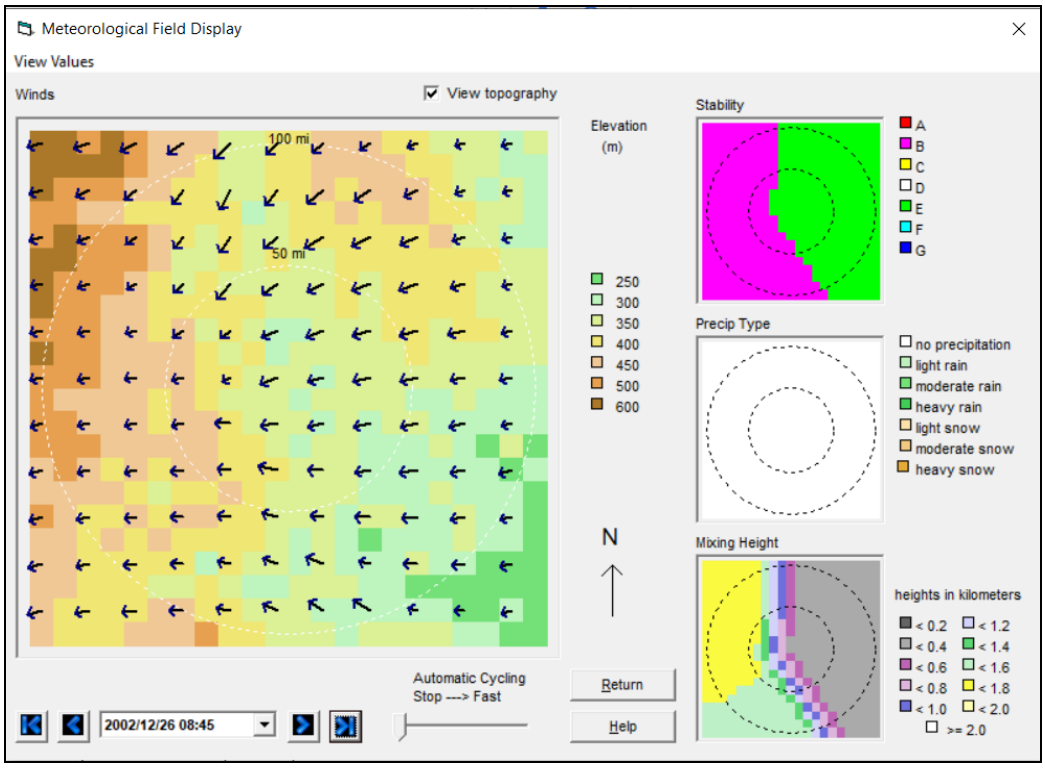

Figure 13: Meteorological data with four-points meteo data, 2002/12/26 08:45 – RASCAL 4.3

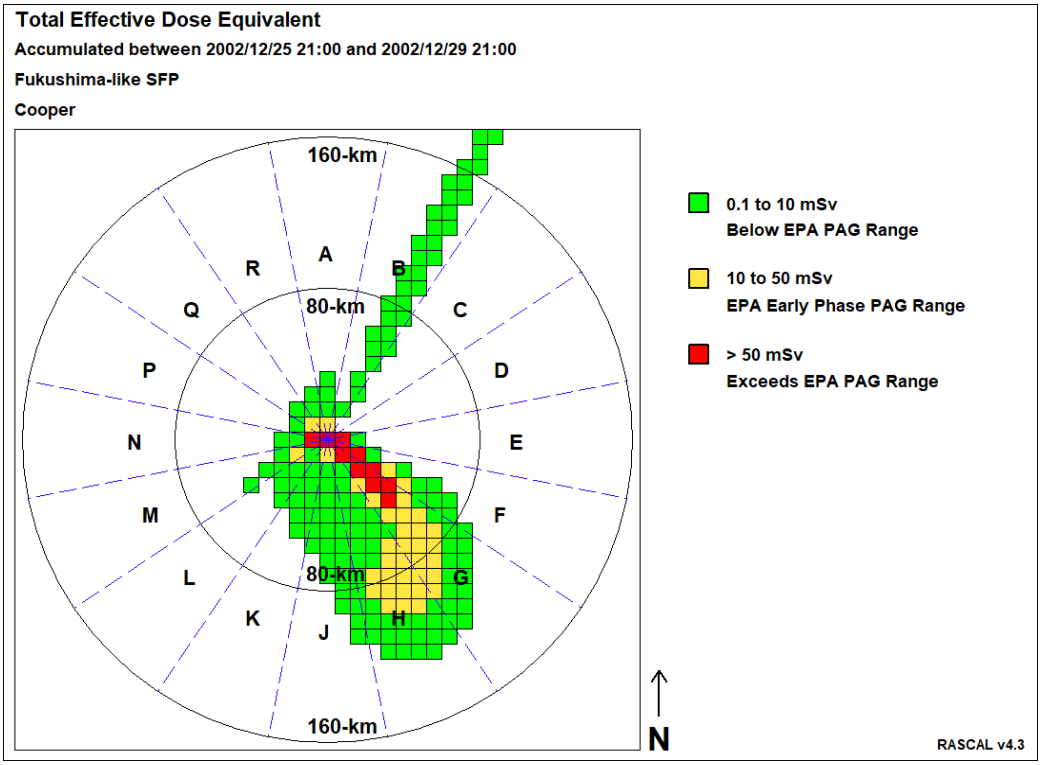

Figure 14: TEDE, one actual 96 hours of meteo data points – RASCAL 4.3

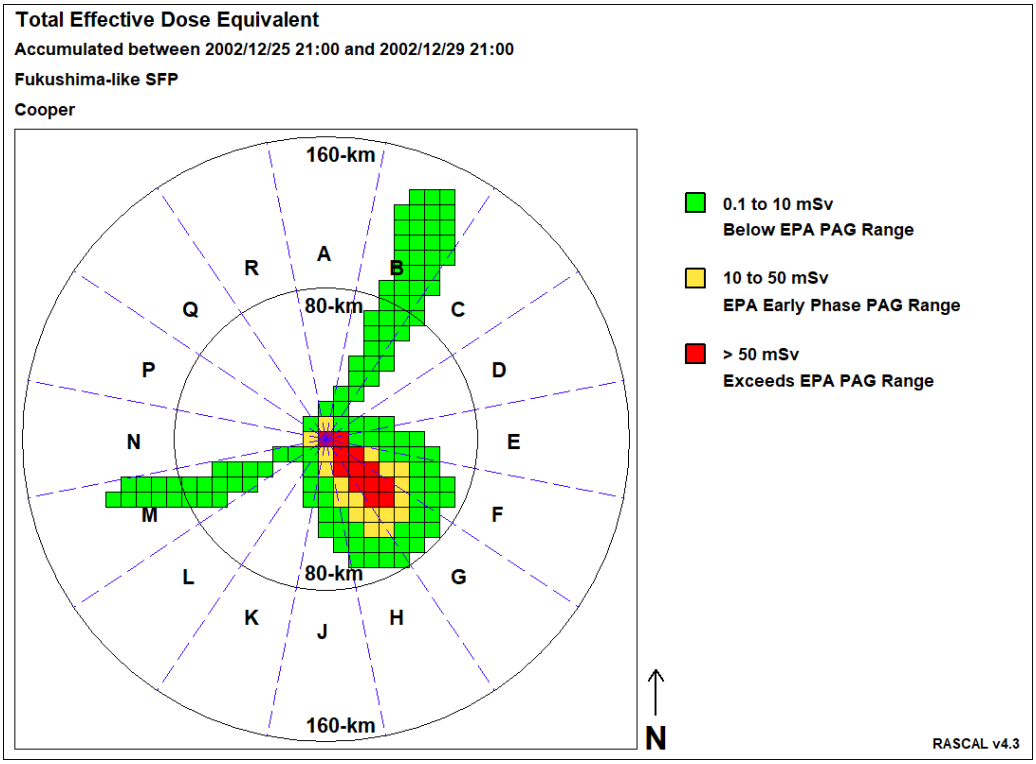

Figure 15: TEDE, four actuals 96 hours of meteo data points – RASCAL 4.3

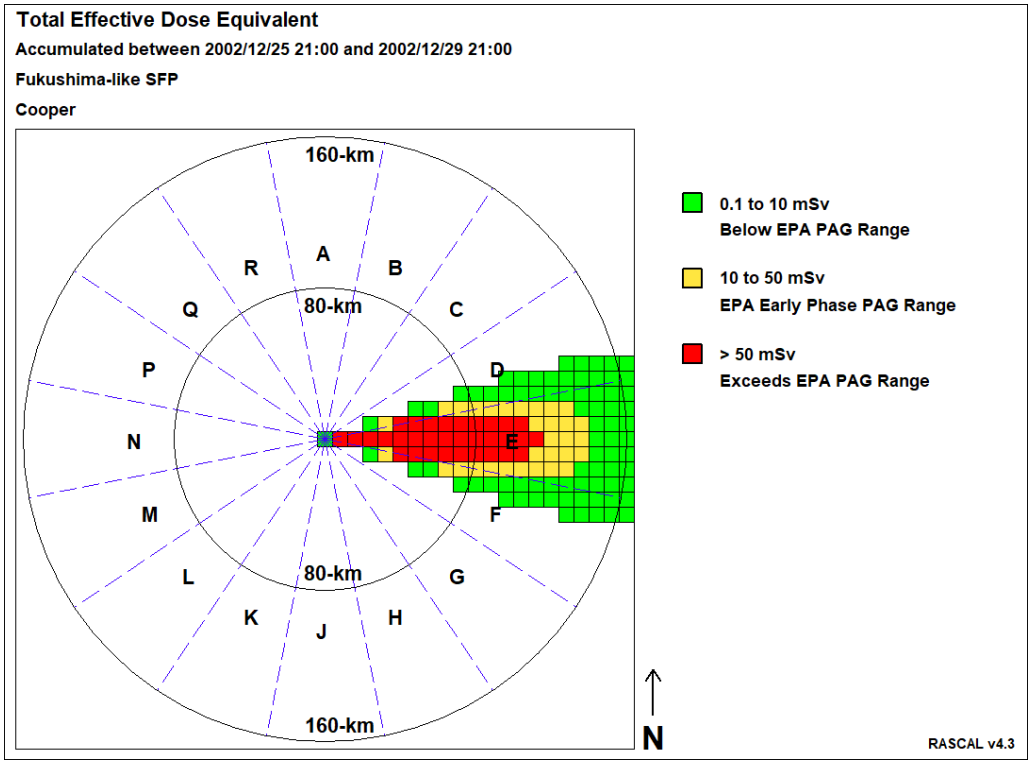

Figure 16: TEDE, standard meteorology – RASCAL 4.3

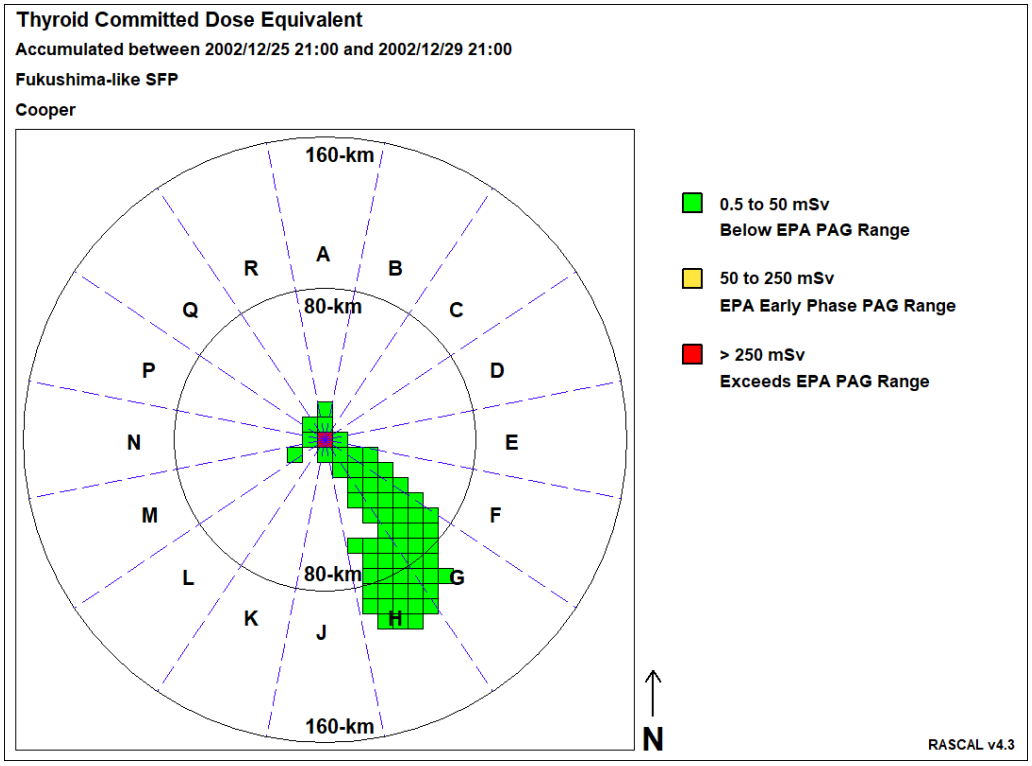

Figure 17: Thyroid dose maps with one point of actual 96 hours of meteo data – RASCAL 4.3

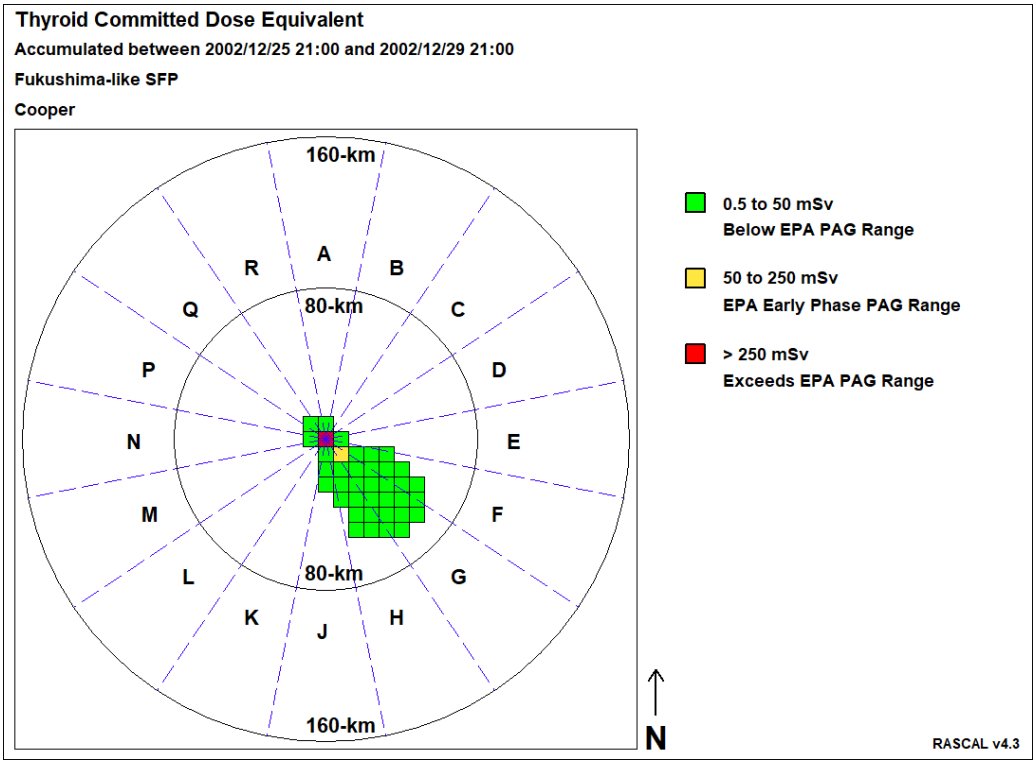

Figure 18: Thyroid dose maps with four points of actual 96 hours of meteo data –RASCAL 4.3

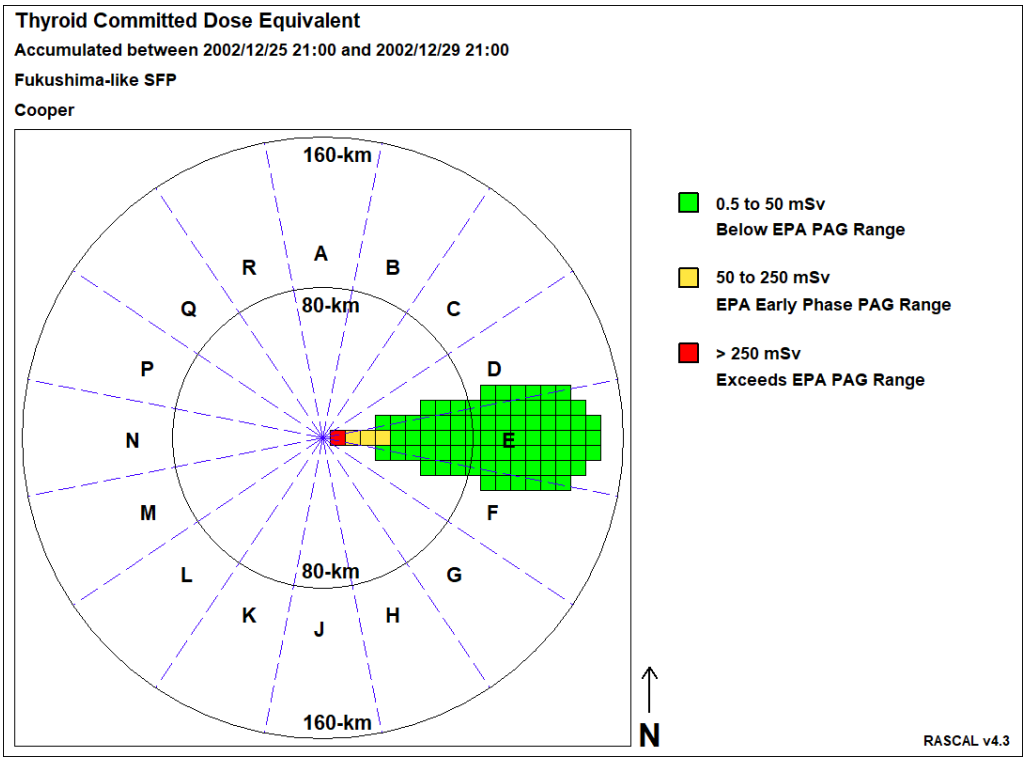

Figure 19: Thyroid dose maps with a standard meteorology – RASCAL 4.3

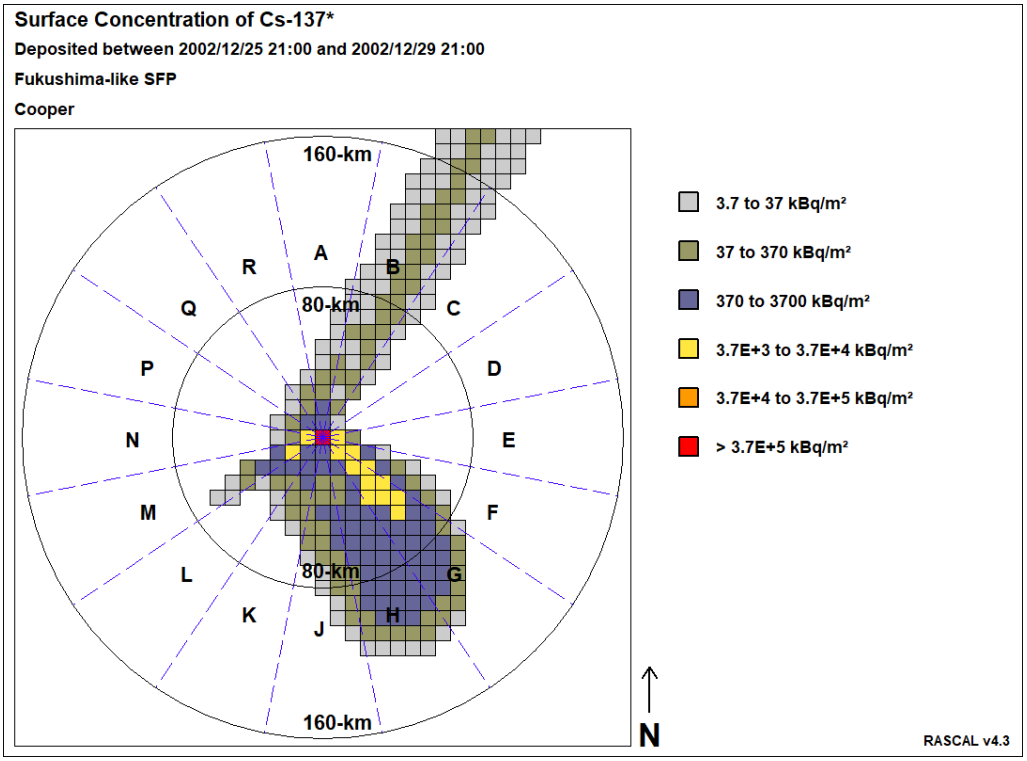

Figure 20: Cs-137 Ground deposition map for one point of actual hourly meteo data – RASCAL 4.3

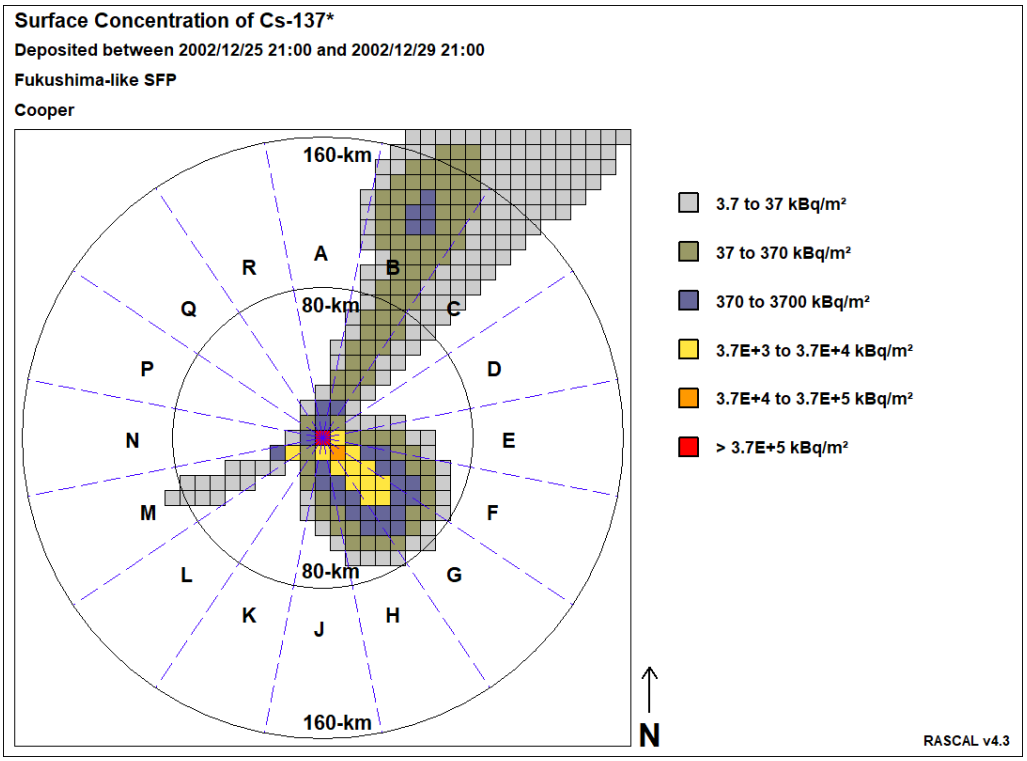

Figure 21: Cs-137 Ground deposition map for four points of actual hourly meteo data – RASCAL 4.3

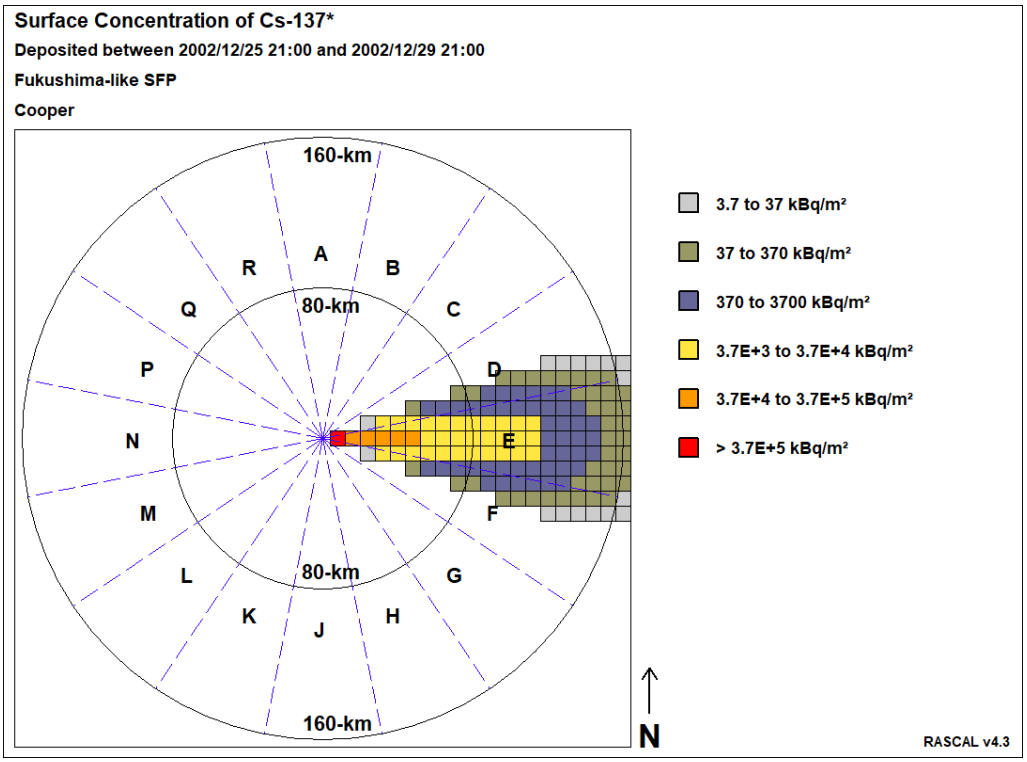

Figure 22: Cs-137 Ground deposition maps for constant standard meteo data – RASCAL 4.3

Table 1: Value of the standard weather parameters, RASCAL 4.3

Date (dd/mm/yyyy)	Wind Speed (m/s)	Wind direction (degree)	Precipitation (m/s)	Surface Temperature (K)	Stability Class
25-29/12/2002	1.8	90.0	0.0	294.2	D

Table 2: Value of the actual hourly weather parameters, location: SFP site

Date (yyyy-mm-dd)	Hour (hh:mm)	Wind speed (m/s)		Wind direction (degree)	Precipitation (m/s)	Surface Temperature (K)	Stability Class
		Average (2700 s)	Gust (900 s)				
2002-12-25	21:00	3.3	4.6	65.1	0	265.2	D
2002-12-25	22:00	3.3	4.5	63.4	2.8x10-8	264.2	D
2002-12-25	23:00	3.1	4.9	61.6	2.8x10-8	264.2	D
…		…	…	…	…	…	
2002-12-29	19:00	1.7	4.3	170.1	0	337.2	E
2002-12-29	20:00	1.7	5.1	185.0	0	296.2	F
2002-12-29	21:00	1.9	4.7	187.0	0	291.2	E

Table 3: Values of the hourly weather data – North point: 70 km away from NPP site, +20° from Central point (source: ERA5 meteo data)

Date	Hour	Wind speed	Wind direction	Precipitation	Temperature	Stability Class
(yyyy-mm-dd)	(hh:mm)	(m/s)	(degree)	(m/s)	(K)	(-)
2002-12-25	21:00	2.1	84.6	0.0	298.2	D
2002-12-25	22:00	1.9	81.0	0.0	301.2	D
2002-12-25	23:00	1.9	78.1	0.0	301.2	D
…	…	…	…	…	…	…
2002-12-29	19:00	1.3	225.0	0.0	253.2	D
2002-12-29	20:00	1.4	225.0	0.0	262.2	F
2002-12-29	21:00	1.5	233.1	0.0	261.2	D

Table 4: Values of the hourly weather data – Central point: 70 km away from NPP site, (source: ERA5 meteo data)

Date	Hour	Wind speed	Wind direction	Precipitation	Temperature	Stability Class
(yyyy-mm-dd)	(hh:mm)	(m/s)	(degree)	(m/s)	(K)	(-)
2002-12-25	21:00	2.2	76.6	0	303.2	D
2002-12-25	22:00	2.1	76.0	0	306.2	D
2002-12-25	23:00	2.1	73.3	0	306.2	D
…	…	…	…	…		…
2002-12-29	19:00	1.4	213.7	0	260.2	D
2002-12-29	20:00	1.6	217.6	0	269.2	F
2002-12-29	21:00	1.8	222.7	0	267.2	D

Table 5: Values of the hourly weather data – South point: 70 km away from SFP site, -20° from Central point (source: ERA5 meteo data)

Date	Hour	Wind speed	Wind direction	Precipitation	Temperature	Stability Class
(yyyy-mm-dd)	(hh:mm)	(m/s)	(degree)	(m/s)	(°C)	(-)
2002-12-25	21:00	1.8	73.6	0.0	309.2	D
2002-12-25	22:00	1.8	73.6	0.0	310.2	D
2002-12-25	23:00	1.7	72.6	0.0	310.2	D
…	…	…	…	…	…	…
2002-12-29	19:00	1.4	219.3	0.0	244.2	D
2002-12-29	20:00	1.7	220.2	0.0	257.2	F
2002-12-29	21:00	1.8	222.7	0.0	262.2	D

Table 6: Time required to perform RC analysis with different set of meteo data

Set of meteorology data (-)	Computational time (s)
Standard meteorology (One point of time independent meteo data)	2100
NPP site related meteorology (One point of actual 96 h meteo data)	2880
NPP site related meteorology (Four points of actual 96 h meteo data)	6180

Table 7: Summary of ST and RC cases analyzed with the associate parameter's options

<table>
<tr><th rowspan="2">Case</th><th colspan="3">ST</th><th colspan="3">RC</th></tr>
<tr><th>Nuclides</th><th>Spray</th><th>Time frame</th><th>Meteodata</th><th>Physical/dosimetric quantities</th><th>Time frame</th></tr>
<tr><td>1</td><td rowspan="3">Cs-134, Cs-136, Cs-137, I-131, Kr-85, Pu-238, Ru-106, Sr-90, Y-90</td><td>No</td><td rowspan="6">96 hours since the start of the atmospheric emission</td><td>Standard</td><td rowspan="3">TEDE, Thyroid dose, Cs-137 ground deposition</td><td rowspan="3">96 hours of atmospheric transport</td></tr>
<tr><td>2</td><td>No</td><td>Hourly, one point</td></tr>
<tr><td>3</td><td>No</td><td>Hourly, four points</td></tr>
<tr><td>4</td><td>I-131</td><td>Yes, pH=4</td><td colspan="3" rowspan="3">No RC evaluation</td></tr>
<tr><td>5</td><td>I-131</td><td>Yes, pH=7</td></tr>
<tr><td>6</td><td>I-131</td><td>Yes, pH=10</td></tr>
</table>

Disclaimer

Views and opinions expressed in this paper reflect only the author's view and the European Commission is not responsible for any use that may be made of the information it contains.